Cholesteric-nematic transition induced by a magnetic field in the strong-anchoring model

Antonio Maria Scarfone,[1] Ioannis Lelidis,[2,3] and Giovanni Barbero[3,4]

[1]*ISC–CNR, Istituto dei Sistemi Complessi, Consiglio Nazionale delle Ricerche, c/o Dipartimento di Fisica del Politecnico di Torino, Corso Duca degli Abruzzi 24, I-10129 Torino, Italy*

[2]*Solid State Section, Department of Physics, University of Athens, Panepistimiopolis, Zografos, Athens GR-157 84, Greece*

[3]*Université de Picardie Jules Verne, Laboratoire de Physique des Systemes Complexes, 33 rue Saint-Leu F-80039, Amiens, France,*

[4]*Dipartimento di Fisica del Politecnico di Torino Corso Duca degli Abruzzi 24, I-10129 Torino, Italy*

(Received 9 May 2011; revised manuscript received 21 July 2011; published 23 August 2011)

We investigate the cholesteric-nematic transition induced by an external bulk field in a sample of finite thickness ℓ. The analysis is performed by considering a tilted magnetic field with respect to the easy direction imposed by rigid boundary conditions inducing planar orientation. In the case of parallel orientation between the magnetic field and of the easy direction, in the limit of $\ell \to \infty$ we reobtain the results of de Gennes where the effective pitch of the cholesteric is a continuous function of the magnetic field diverging at the critical field related to the cholesteric-nematic transition. For finite ℓ we obtain a cascade of transitions, where the bulk expels a half-pitch at a time to avoid divergences in the elastic energy, in a similar manner as solids expel defects in the presence of strong deformation. In the case of oblique orientation between the magnetic field and the easy direction, only the completely untwisted state depends on the tilt angle. Therefore, only the cholesteric-nematic transition depends on the tilt angle while all the other magnetic transition values are unchanged.

DOI: 10.1103/PhysRevE.84.021708 PACS number(s): 61.30.Dk, 64.70.M−

I. INTRODUCTION

The spontaneous twisted arrangement of the molecules in cholesteric liquid crystals (CLCs) is at the origin of their unique electro-optical and photonic properties [1–3] such as selective reflection, flexoelectricity, photonic band edge lasing, etc., that are widely used in many device applications (displays, thermometers, optical storage, laser, etc.). These properties may be tuned by modifying reversibly the pitch of the helix with an electric or magnetic field, the temperature, and light irradiation.

The effect of an external bulk (magnetic or electric) field on helix unwinding of cholesteric liquid crystals has been described theoretically by de Gennes [4] and independently by Meyer [5] in the case of an infinite (unbounded) sample (free boundary conditions). The untwist of the cholesteric under magnetic field perpendicular to the helical axis has been observed by using the NMR technique [6] and by a dc electric field [7]. The variation of the cholesteric pitch on the bulk field strength and the critical field for the helix unwinding have been measured by direct optical observations using a magnetic field [8,9] and an electric field [10]. Other aspects of the model such as the critical field dependence on the undisturbed cholesteric pitch [11] and the dielectric anisotropy [12] have been also experimentally verified. In the case of a bounded sample with rigid anchoring conditions Dreher [13] predicted that the pitch of the CLC can change only stepwise by a magnetic field. The step unwinding of a CLC by a nonuniform electric field has been optically observed using the Grandjean-Cano texture [14]. The cholesteric π walls dynamics is analyzed in Ref. [15], while a stability analysis of the pitch transition has been developed in Ref. [16]. The more complex case of a surface field-induced unwinding has also been analyzed [17,18]. The problem of the helix unwinding in CLCs by a bulk field has been further reconsidered theoretically [19–24] and experimentally [25–33]. Nevertheless it has not been elucidated in all of its aspects. Note that the same problem appears also in smectic ferroelectric liquid crystals [34]. In fact, the helix distortion or complete unwinding is a common problem in a variety of domains in condensed matter physics and biophysics [35–37].

Previous studies on CLCs unwinding in a bounded sample have focused on an external bulk field perpendicular to the helical axis and to the easy direction imposed by the anchoring conditions [13,19,20]. The axis of the helix is either parallel to the substrate or perpendicular to it. The present article focuses on the cholesteric helix deformation and unwinding of a bounded sample by a magnetic field in the general case where the external field is orthogonal to the helix axes but it makes an arbitrary angle with the easy orientation imposed by rigid planar anchoring on the cell plates (tilted configuration). In our analysis we consider a one-dimensional deformation of pure twist induced by the field in the cell of CLCs with Grandjean texture and isothermal conditions. First, we analyze the case of an external bulk field parallel to the easy direction, and we calculate (1) the deformation of the initially harmonic helix by the field that takes place at constant pitch and its stepwise unwinding, (2) the relative free-energy variation that depends on the half-pitch number as a function of the field strength, (3) the nematic director profile in the cell that becomes asymmetric for the tilted configuration, and (4) the cholesteric-nematic (Ch-N) transition diagram. Further we demonstrate that the critical field for pitch transitions does not depend on the tilt between the easy anchoring direction and the magnetic field, but the complete helix unwinding does depend on it. Finally, a supercritical bifurcation is revealed in the case of a field perpendicular to the easy direction of the nematic director.

The layout of the article is as follows. In Sec. II we reconsider the problem for a magnetic field parallel to the alignment direction. In Sec. III we present the generalization of the model for a tilted magnetic field in respect to the anchoring easy direction. Finally, Sec. IV is devoted to discussion and conclusions.

II. MAGNETIC FIELD PARALLEL TO THE IMPOSED EASY DIRECTIONS

Let us consider a sample in the shape of a slab of thickness $\ell = N\Lambda$, where Λ is the cholesteric half-pitch, under the influence of a magnetic field parallel to the easy direction imposed by the surface treatment. The Cartesian reference frame used in the description has the z axis perpendicular to the surfaces limiting the sample, located at $z = 0$ and $z = \ell$. The surface easy directions are parallel to the y axis, such that $\boldsymbol{n}(0) = \boldsymbol{n}(\ell) = \boldsymbol{j}$, where $\boldsymbol{n}$ is the nematic director and $\boldsymbol{j}$ is the unit vector along the y axis. The magnetic field is assumed in the $\boldsymbol{j}$ direction so that $\boldsymbol{H} = H\,\boldsymbol{j}$.

It is useful to rescale the z coordinate as $\zeta = z/\ell$ in such a manner that $0 \leqslant \zeta \leqslant 1$. We denote by $\lambda = \Lambda/\ell = 1/N$ the density of π twist in the sample, representing the number of π twists per unit length in the absence of magnetic field.

In the ground state, where $\boldsymbol{H} = \boldsymbol{0}$, the cholesteric liquid crystal presents only a twist deformation defined by a twist angle $\phi_N(z) = (\pi/\Lambda)\,z \equiv (\pi/\lambda)\,\zeta$, where ϕ_N is the angle formed by $\boldsymbol{n}$ with the y axis. On the other hand, in the presence of $\boldsymbol{H} \neq \boldsymbol{0}$, ϕ_N is modified in ϕ_n, with $n = N, N-1, \ldots, 0$, according to the intensity of $\boldsymbol{H}$.

The actual ϕ_n profile is the one minimizing the total energy per unit surface of the cholesteric liquid crystal, given by

$$G_n = \frac{K}{2}\int_0^{\ell}\left[\left(\frac{d\phi_n}{dz} - \frac{\pi}{\Lambda}\right)^2 - \frac{1}{\Xi^2}\cos^2(\phi_n)\right]dz, \tag{2.1}$$

with the boundary conditions $\boldsymbol{n}(0) = \boldsymbol{n}(\ell) = \boldsymbol{j}$. In Eq. (2.1), K is the twist elastic constant, $\Xi = \sqrt{K/\chi_a H^2}$ is the magnetic coherence length, and $\chi_a = \chi_{\parallel} - \chi_{\perp}$, where $\parallel$ and $\perp$ refer to $\boldsymbol{n}$, is the diamagnetic anisotropy.

After rescaling the free energy (2.1), we can consider equivalently the dimensionless function $\mathcal{G}_n = (2\,\ell/K)\,G_n$ given by

$$\mathcal{G}_n = \int_0^1\left[\left(\varphi_n' - \frac{\pi}{\lambda}\right)^2 - \frac{1}{\xi^2}\cos^2(\varphi_n)\right]d\zeta, \tag{2.2}$$

where $\varphi_n(\zeta) \equiv \phi_n(z)$, $\varphi_n' = d\varphi_n/d\zeta$, and $\xi = \Xi/\ell$.

The function φ_n minimizing $\mathcal{G}_n$ is solution of the following differential equation:

$$\varphi_n'' - \frac{1}{\xi^2}\sin(\varphi_n)\cos(\varphi_n) = 0 \tag{2.3}$$

and can be rewritten as

$$\varphi_n'^2 - \frac{1}{\xi^2}\sin^2(\varphi_n) = \frac{k_n}{\xi^2}, \tag{2.4}$$

where $k_n \equiv k_n(\xi)$ has to determined by means of the boundary conditions related to the strong anchoring hypothesis on the limiting surfaces.

In the limit $\boldsymbol{H} \to \boldsymbol{0}$, i.e., when $\xi \to \infty$, $\varphi_n \to \varphi_N$, and $\varphi_N' \to \pi/\lambda$. In the same limit, from Eq. (2.4), we get

$$\lim_{\xi\to\infty}\frac{k_n}{\xi^2} = \left(\frac{\pi}{\lambda}\right)^2. \tag{2.5}$$

By means of Eq. (2.4) we obtain

$$\varphi_n' = \pm\frac{1}{\xi}\sqrt{k_n + \sin^2(\varphi_n)}, \tag{2.6}$$

where signs refer to the two possible elicit states of molecule. Hereinafter we assume the levogyre direction (+). The general solution of Eq. (2.6) is

$$\frac{\zeta}{\xi} = \mathcal{F}(\varphi_n, k_n), \tag{2.7}$$

where

$$\mathcal{F}(\varphi, k) = \int_0^{\varphi}\frac{d\alpha}{\sqrt{k + \sin^2(\alpha)}}. \tag{2.8}$$

The function $\mathcal{F}(\varphi, k)$ is related to the elliptic integral of the first kind according to $F(\phi, \kappa) = \sqrt{k}\,\mathcal{F}(\varphi, k)$, with $\kappa^2 = -1/k$.

Accounting for the boundary conditions $\varphi_n(0) = 0$ and $\varphi_n(1) = n\,\pi$, we get k_n by means of the implicit equation

$$\mathcal{F}(n\,\pi, k_n) = \frac{1}{\xi}. \tag{2.9}$$

Furthermore, recalling the periodicity of $F(\varphi, \kappa)$ we have $\mathcal{F}(n\,\pi, k_n) = n\,\mathcal{F}(\pi, k_n)$, so that Eq. (2.9) becomes

$$\mathcal{F}(\pi, k_n) = \frac{1}{n\,\xi}. \tag{2.10}$$

In Fig. 1 we show ξ versus k_n for several values of the twist numbers n. We note that ξ vanishes for $k_n \to 0$ according to

$$\xi = \frac{1}{n\,(4\,\ln 2 - \ln k_n)} + \frac{O(k_n)}{\ln k_n}, \tag{2.11}$$

although $\lim_{\xi\to 0} k_n/\xi \to 0$. In the opposite direction, for $\xi \to \infty$, Eq. (2.5) is verified.

When k_n is known, we can derive implicitly the twist angle profile φ_n as

$$\frac{\mathcal{F}(\varphi_n, k_n)}{\mathcal{F}(\pi, k_n)} = n\,\zeta. \tag{2.12}$$

The total energy (2.2) can be rewritten as

$$\begin{aligned}\mathcal{G}_n &= \int_0^{n\,\pi}\left[\left(\varphi_n' - \frac{\pi}{\lambda}\right)^2 - \frac{1}{\xi^2}\cos^2(\varphi_n)\right]\frac{d\varphi_n}{\varphi_n'} \\ &= \frac{2\,n}{\xi}\,\mathcal{E}(\pi, k_n) - 2\,\frac{n\,\pi^2}{\lambda} + \left(\frac{\pi}{\lambda}\right)^2 - \frac{1}{\xi^2}\,(1 + k_n),\end{aligned} \tag{2.13}$$

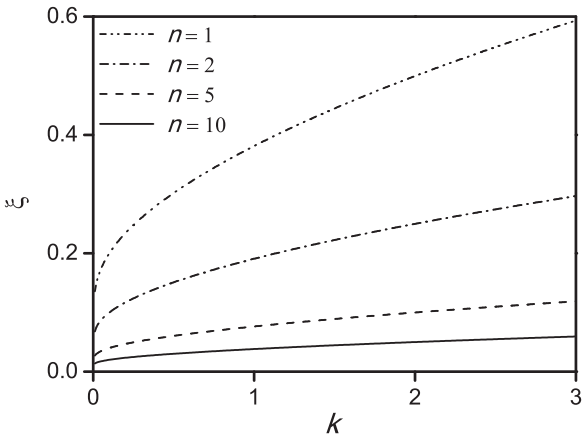

FIG. 1. Plot of ξ vs k_n for several values of the half-twist numbers n. We note that ξ vanishes for $k_n \to 0$ although $\lim_{\xi\to 0} k_n/\xi = 0$.

where the function

$$\mathcal{E}(\varphi, k) = \int_0^{\varphi} \sqrt{k + \sin^2(\alpha)}\, d\alpha \tag{2.14}$$

is related to the elliptic integral of the second kind.

Let us consider first the natural state occurring for $\boldsymbol{H}$ quite small, where $n = N$. In this situation k_N is given by

$$\mathcal{F}(\pi, k_N) = \frac{\lambda}{\xi}, \tag{2.15}$$

and the tilt angle profile can be derived from the relation

$$\frac{\mathcal{F}(\varphi_N, k_N)}{\mathcal{F}(\pi, k_N)} = \frac{\zeta}{\lambda}. \tag{2.16}$$

The total energy per unit surface is

$$\mathcal{G}_N = N\left[\frac{2}{\xi}\,\mathcal{E}(\pi, k_N) - 2\,\frac{\pi^2}{\lambda}\right] + \left(\frac{\pi}{\lambda}\right)^2 - \frac{1}{\xi^2}\,(1 + k_N). \tag{2.17}$$

Increasing the magnitude of the magnetic field $\boldsymbol{H}$, i.e., decreasing ξ, the twist angle profile φ_n changes according to Eq. (2.16). This is shown in Fig. 2, where we plot, for the case of $n = 2$, the projection of the nematic direction $\boldsymbol{n}(\zeta)$ along $\boldsymbol{j}$: $n_y(\zeta) = \boldsymbol{n} \cdot \boldsymbol{j}$ [cf. Fig. 2(a)], and the tilt angle $\varphi_2(\zeta)$ [cf. Fig. 2(b)] for several values of ξ. We observe that the present situation differs from the one considered in Ref. [1] for the following reason: In Ref. [1] the case of a unbounded sample is considered, and the cholesteric pitch increases continuously as the magnetic field grows. In that case no boundary conditions are imposed on the twist angle profile. In contrast, in the present case this cannot occur due to the constraints on the boundaries. As shown in Fig. 2(b), increasing the magnetic field the twist angle profile goes toward a step function. In the same limit, as shown in Fig. 2(c), near the points ζ^* where $\varphi_n = \pi/2$, the slope of $\varphi_n(\zeta)$, given by

$$\varphi_n'(\zeta^*) = \frac{1}{\xi}\sqrt{k_n + 1}, \tag{2.18}$$

diverges. Consequently, the elastic energy density, proportional to $[\varphi_n' - (\pi/\lambda)]^2$, diverges too, and the state related to $\varphi_n(\zeta)$ becomes unstable.

The system, to avoid the divergence of the elastic energy, expels a π twist by relaxing in a configuration with lower energy density, containing $n - 1$ twists. The situation is similar, in some manner, to the expulsion of a defect in solid material when the elastic deformation increases. In fact, in the state with $n - 1$ twists, we have

$$\mathcal{F}(\pi, k_{n-1}) = \frac{1}{(n-1)\,\xi}, \tag{2.19}$$

so that

$$\frac{\mathcal{F}(\varphi_{n-1}, k_{n-1})}{\mathcal{F}(\pi, k_{n-1})} = (n-1)\,\zeta, \tag{2.20}$$

from which one obtains the new shape for the tilt angle φ_{n-1}. From Eqs. (2.10), we can obtain

$$n\,\mathcal{F}(\pi, k_n) = (n-1)\,\mathcal{F}(\pi, k_{n-1}), \tag{2.21}$$

which relates k_n with k_{n-1}.

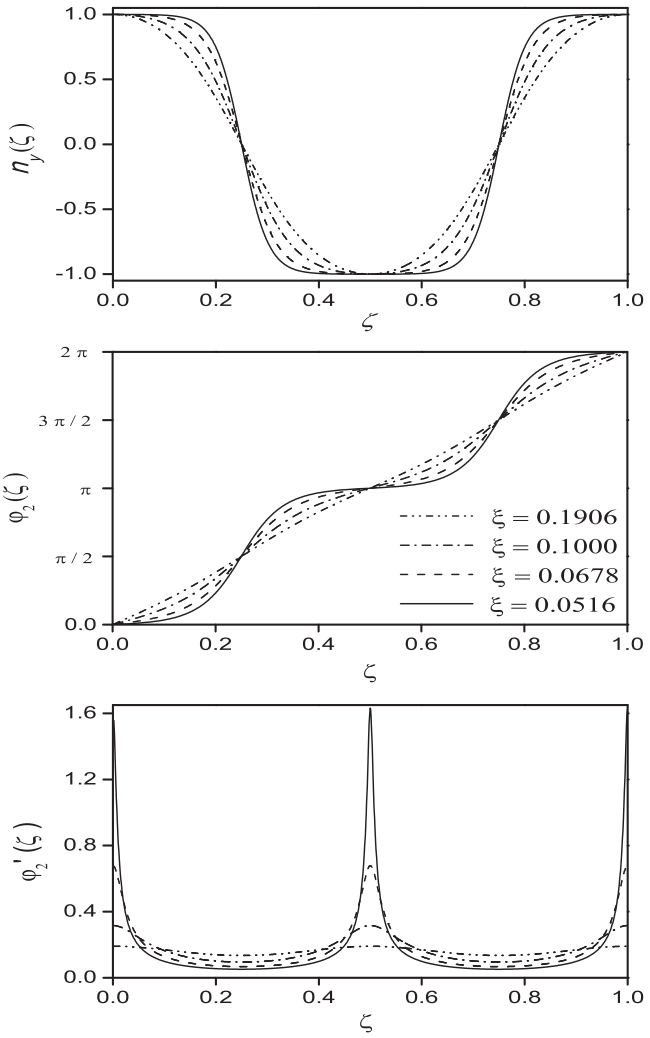

FIG. 2. y component of the nematic direction $n_y(\zeta) = \boldsymbol{n}(\zeta) \cdot \boldsymbol{j}$ vs ζ (a); twist angle $\varphi_2(\zeta)$ vs ζ (b); and gradient of the twist angle $\varphi_2'(\zeta)$ vs ζ (c); for $n = 2$ half-twists and the values of the magnetic field reported in Fig. 1.

As a consequence of transition from n to $n - 1$ twists, the energy density relaxes to

$$\mathcal{G}_{n-1} = (n-1)\left[\frac{2}{\xi}\,\mathcal{E}(\pi, k_{n-1}) - 2\,\frac{\pi^2}{\lambda}\right] + \left(\frac{\pi}{\lambda}\right)^2 - \frac{1}{\xi^2}\,(1 + k_{n-1}). \tag{2.22}$$

In particular, the transition from the state with n twists to the one with $n - 1$ twists takes place when

$$\mathcal{G}_n = \mathcal{G}_{n-1}, \tag{2.23}$$

and, by taking into account Eqs. (2.17) and (2.22) it can be rewritten as

$$\frac{2}{\xi}\,[n\,\mathcal{E}_n(\pi, k_n) - (n-1)\,\mathcal{E}_{n-1}(\pi, k_{n-1})] = 2\,\frac{\pi^2}{\lambda} + \frac{k_n - k_{n-1}}{\xi^2}\,. \tag{2.24}$$

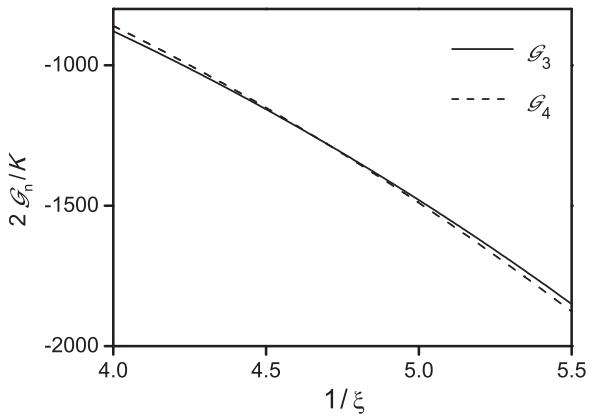

FIG. 3. Dependence of the reduced energy of the cholesteric sample vs $1/\xi \propto |\boldsymbol{H}|$, for $n = 3$ and 4 in the case $N = 4$. The transition $4 \to 3$ takes place at the intersection point between $\mathcal{G}_4$ and $\mathcal{G}_3$.

Its solution gives the critical magnetic field where the transition $n \to n-1$ occurs. This is depicted in Fig. 3, where we show the $\mathcal{G}_4$ and $\mathcal{G}_3$ versus $1/\xi \propto |\boldsymbol{H}|$, for the case $N = 4$.

This process occurs recursively as the magnetic field increases so that, whenever it reaches the critical values obtained from the above equation, after replacing N with $N-1, N-2, \ldots, 1$, the system evolves to a more stable configuration by reducing its number of π twists.

Let us examine in detail the last transition that takes place when the number of twists passes from $n = 1$ to $n = 0$, i.e., the cholesteric-nematic transition. In the state where the cholesteric sample presents just one twist, the twist angle profile φ_1 is given by

$$\mathcal{F}(\pi, k_1) = \frac{1}{\xi}, \tag{2.25}$$

$$\frac{\mathcal{F}(\varphi_1, k_1)}{\mathcal{F}(\pi, k_1)} = \zeta, \tag{2.26}$$

and the energy density becomes

$$\mathcal{G}_1 = \frac{2}{\xi}\,\mathcal{E}(\pi, k_1) - 2\,\frac{\pi^2}{\lambda} + \left(\frac{\pi}{\lambda}\right)^2 - \frac{1}{\xi^2}\,(1 + k_1). \tag{2.27}$$

On the contrary, in the state with $n = 0$, $\varphi_0(1) = 0$ according to the boundary conditions, and the sample does not present any twist deformation. In this case, the stable configuration is given by $\varphi_0(\zeta) = 0$, and the relevant total energy per unit surface is

$$\mathcal{G}_0 = \left(\frac{\pi}{\lambda}\right)^2 - \frac{1}{\xi^2}. \tag{2.28}$$

The last transition occurs when $\mathcal{G}_1 = \mathcal{G}_0$; that means

$$\frac{2}{\xi}\,\mathcal{E}(\pi, k_1) - 2\,\frac{\pi^2}{\lambda} - \frac{k_1}{\xi^2} = 0. \tag{2.29}$$

We note that, in the $\ell \to \infty$ limit, the density of twists goes to zero, so that this last equation can be approximated in

$$\frac{\Lambda}{\Xi} = \frac{\pi^2}{\mathcal{E}(\pi, k_1)}, \tag{2.30}$$

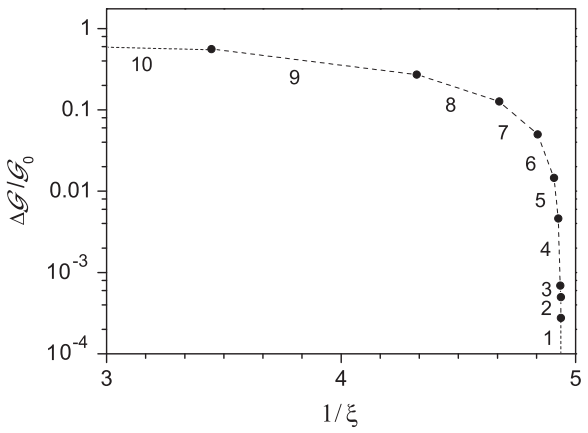

FIG. 4. Cascade of the twist transitions vs $1/\xi \propto \boldsymbol{H}$ in a cholesteric slab of finite thickness for a sample with $N = 10$ twists. Note that the finite thickness of the sample is responsible for a discrete variation of the cholesteric periodicity induced by the magnetic field.

where $\Lambda/\Xi = \lambda/\xi$.

On the other hand, since k_1 tends to zero more rapidly than ξ, as shown in Fig. 1, from the definition (2.14) we have $\lim_{\ell\to\infty} \mathcal{E}(\pi, k_1) \sim 2$, and Eq. (2.30) gives the critical field

$$\frac{1}{\Xi} = \frac{\pi^2}{2\,\Lambda}, \tag{2.31}$$

in accordance with the results derived in Ref. [1] for the cholesteric-nematic transition in a unbounded sample [4].

In Fig. 4 we show the sequence of transitions versus $1/\xi \propto |\boldsymbol{H}|$ in a sample with $N = 10$ twists. In this figure we report on the ordinate the relative energy variation $\Delta\mathcal{G}/\mathcal{G}_0 = (\mathcal{G}_0 - \mathcal{G}_n)/\mathcal{G}_0$ where $\mathcal{G}_0$ is the energy density of the final state. Figure 5 shows the diagram of the N-Ch transition in the plane of the critical field $1/\xi_c \propto |\boldsymbol{H}_c|$ for complete unwinding of the helix versus $1/\lambda$ that is proportional to the confinement ratio usually defined as $\ell/2\,\Lambda$ [23]. For large values of $1/\lambda$ the critical field goes asymptotically to the de Gennes prediction (dashed line). When the confinement ratio reduces, the surface field

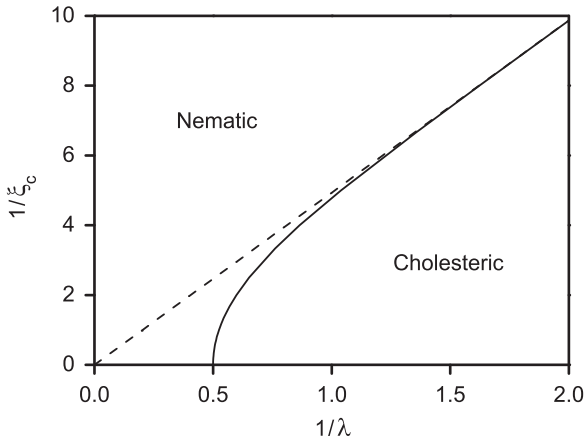

FIG. 5. Diagram of the N-Ch transition in the plane $1/\xi_c \propto |\boldsymbol{H}_c|$ vs $1/\lambda$. The solid line corresponds to the N-Ch transition in confined geometry and rigid boundary conditions. The dashed line is the asymptote of the transition line for large values of the confinement ratio.

due to the rigid boundary condition adds to the external bulk field, and the contribution of the latter in the transition reduces continuously toward zero at a critical value of the confinement ratio $1/\lambda_c$, where λ_c denotes the value of λ at the crossing point of the transition line with the axis $1/\xi_c = 0$. For values of $1/\lambda \leqslant 1/\lambda_c$ the cholesteric is reduced to the nematic phase from the action of the surface field alone. In fact, the action of a surface field combined with an external bulk field at transitions in liquid crystals is well known [38]. In cholesteric LCs, it has been studied particularly in homeotropic geometry [32]. We have fitted the numerically calculated transition line with the following scaling-law expression:

$$\frac{1}{\xi_c} \sim \left(\frac{1}{\lambda} - \frac{1}{\lambda_c}\right)^x. \tag{2.32}$$

Here $\lambda_c = 2$ is calculated analytically from (2.29). The value of the exponent x tends to 0.5 as λ goes toward λ_c, while for large values of the confinement ratio the exponent goes to the value $x = 1$, in agreement with de Gennes's prediction (see (2.31)). These values can be calculated analytically from an asymptotic analysis of (2.29).

Asymptotic expansion of the elliptic integrals $\mathcal{E}(\pi, k_1)$ and $\mathcal{F}(\pi, k_1)$ about $k_1 = \infty$ gives

$$\mathcal{E}(\pi, k_1)/\pi = k_1^{1/2} + \tfrac{1}{4}\, k_1^{-1/2} - \tfrac{3}{64}\, k_1^{-3/2} + \mathcal{O}\big(k_1^{-5/2}\big), \tag{2.33}$$

$$\mathcal{F}(\pi, k_1)/\pi = k_1^{-1/2} - \tfrac{1}{4}\, k_1^{-3/2} + \mathcal{O}\big(k_1^{-5/2}\big). \tag{2.34}$$

Thus upon combining the latter expansions and (2.29) we obtain

$$\frac{1}{\lambda} - \frac{1}{\lambda_c} = \frac{1}{4}\, k_1^{-1} + \mathcal{O}\big(k_1^{-2}\big). \tag{2.35}$$

Finally, introducing ξ from (2.25), we obtain the scaling law for the magnetic field dependence on the confinement ratio

$$\frac{1}{\xi_c} = 2\pi \left(\frac{1}{\lambda} - \frac{1}{\lambda_c}\right)^{1/2}. \tag{2.36}$$

The numerical value of the exponent x is in good agreement with its analytic value. Equation (2.36) can also be obtained by expanding the free energy (2.2) in power series of the wave number and can make a Landau expansion to determine the shift in the critical field due to the finite dimension of the sample.

III. GENERALIZATION OF THE PROBLEM TO THE TILTED SITUATION

We generalize the above problem by considering the tilted configuration, where the magnetic field is tilted with respect to the easy direction imposed by the surfaces treatment. To be explicit, let us consider a sample made by a sample in the slab of thickness $\ell = N\,\Lambda$ whose surface easy directions are still parallel to the y axis, like $\boldsymbol{n}(0) = \boldsymbol{n}(\ell) = \boldsymbol{j}$, but now the magnetic field $\boldsymbol{H} = H[\boldsymbol{i}\,\sin(\varphi_H) + \boldsymbol{j}\,\cos(\varphi_H)]$, where φ_H is the angle that the magnetic field makes with the orientation

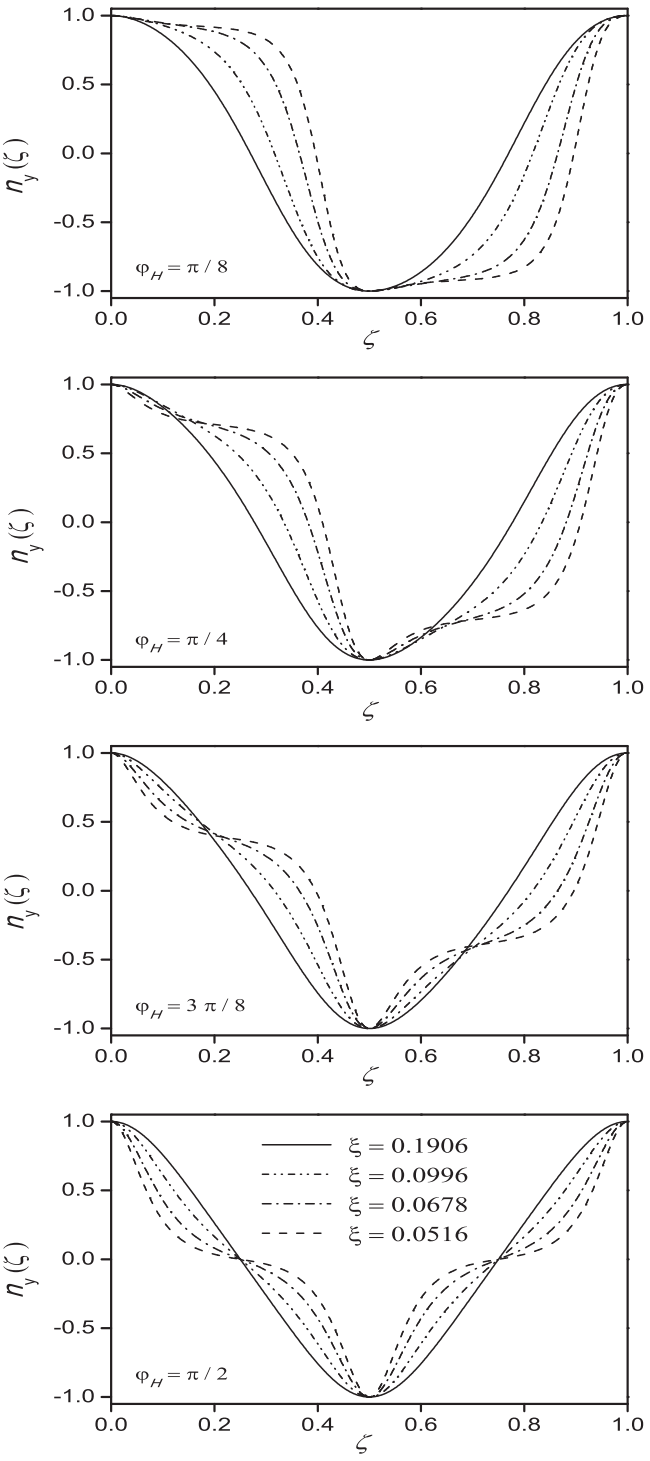

FIG. 6. y direction of the nematic direction $n_y(\zeta)$ for several values of φ_H and of ξ, for the case $n = 2$.

imposed by the surface treatment. The total energy per unit surface becomes

$$\mathcal{G}_n = \int_0^1 \left[\left(\varphi_n' - \frac{\pi}{\lambda}\right)^2 - \frac{1}{\xi^2}\,\cos^2(\varphi_n - \varphi_H)\right] d\zeta, \tag{3.1}$$

and the boundary conditions on the twist angle are $\varphi_n(0) = 0$ and $\varphi_n(1) = n\,\pi$ where $n = N, N-1, \ldots, 0$.

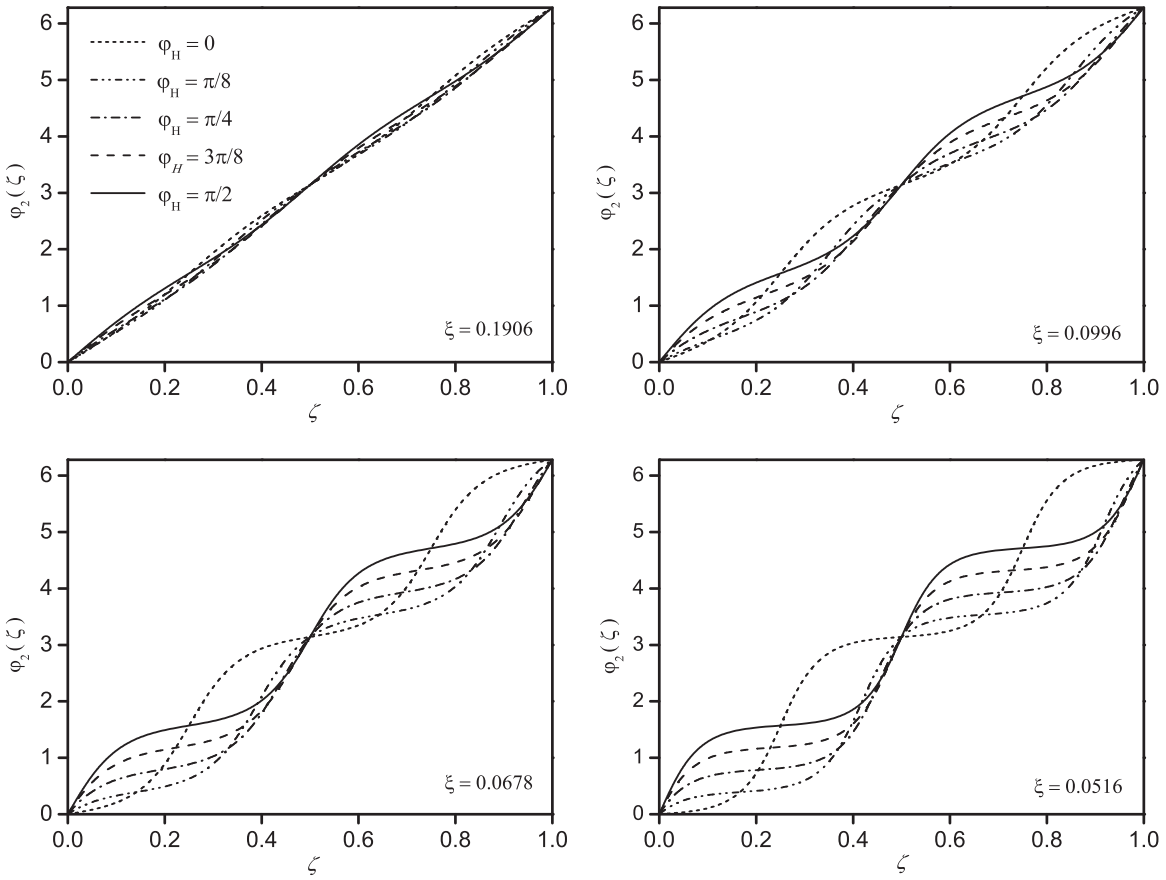

FIG. 7. Twist angle for the values of ξ and φ_H corresponding to the cases depicted in Fig. 6.

Following step by step the analysis presented in the previous section we obtain

$$\varphi_n' = \frac{1}{\xi}\sqrt{k_n + \sin^2(\varphi_n - \varphi_H)}, \tag{3.2}$$

where we kept the levogyre direction (+) as previously. For $n > 0$, k_n is still defined as

$$\mathcal{F}(\pi, k_n) = \frac{1}{n\,\xi}. \tag{3.3}$$

This equation shows that k_n is independent of φ_H. In the same way, the tilt angle profile is given by

$$\frac{\mathcal{F}(\varphi_n, k_n)}{\mathcal{F}(\pi, k_n)} = n\,\zeta, \tag{3.4}$$

which coincides with Eq. (2.12) since, according with Eq. (3.3), the energy density does not depend on φ_H whenever $n > 0$.

In Fig. 6 we plot, for the case $n = 2$, the director component $n_y(\zeta) = \boldsymbol{n}\cdot\boldsymbol{j}$ for several values of φ_H and ξ. We notice that the presence of a different orientation of $\boldsymbol{H}$ induces a sustaining in the shape of $\boldsymbol{n}$ that is emphasized by the growth of the intensity of $\boldsymbol{H}$. We also highlight the symmetry of the shape of $\boldsymbol{n}(\zeta)$ as a consequence of the invariance of the system under the angle translation $\varphi_n(\zeta) \to \varphi_n(\zeta) + \pi$. This is clear from Fig. 7, where we plotted the twist angle for the same cases depicted in Fig. 6.

We note that, in spite of the different boundary conditions, Eqs. (2.13) and (3.1) give the same numerical value since both integrals are evaluated over n complete periods. As a consequence Eq. (2.23) is satisfied at the same critical field value. This means that the critical value of the magnetic field corresponding, respectively, to the transitions $N \to N-1 \to \cdots \to 1$ is not affected by the angle φ_H.

In order to investigate the final transition $1 \to 0$, let us consider now the state $n = 0$ where there is not complete twist. From the boundary condition $\varphi_0(0) = \varphi_0(1) = 0$ it follows that there exists a point ζ^* where $\varphi'(\zeta^*) = 0$. For the symmetry of the problem this point must be located at $\zeta^* = 1/2$. We can account for this condition by imposing

$$\varphi_0'(1/2) = \frac{1}{\xi}\sqrt{k_0 + \sin^2(\varphi_M - \varphi_H)} = 0, \tag{3.5}$$

where $\varphi_M = \varphi_0(1/2)$ corresponds to the maximal deformation of the twist angle with respect to the anchoring directions. From the above equation we get

$$k_0 = -\sin^2(\varphi_M - \varphi_H), \tag{3.6}$$

and the quantity φ_M can be determined through the relation

$$\int_0^{\varphi_M} \frac{d\varphi}{\sqrt{\sin^2(\varphi - \varphi_H) - \sin^2(\varphi_M - \varphi_H)}} = \frac{1}{2\,\xi}. \tag{3.7}$$

The dependence of φ_M versus ξ for several values of φ_H is depicted in Fig. 8. We observe as increasing the strength of the magnetic field that the twist angle continuously saturates

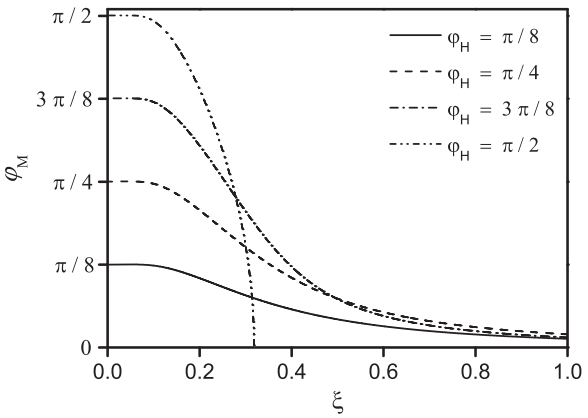

FIG. 8. Dependence of φ_M vs ξ for several values of φ_H. The thin solid curve is drawn for $\lambda = 0.1$.

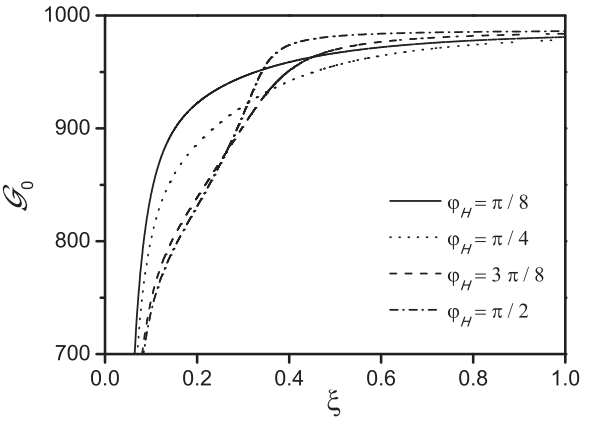

FIG. 10. Total energy per unit surface $\mathcal{G}_0$ for the same values of φ_H reported in the Fig. 8 and for $\lambda = 0.1$.

to φ_H. In particular, the curve $\varphi_H = \pi/2$ shows an abrupt but continuous variation of the twist angle above a critical field typical of a second-order phase transition. Since the nematic director is apolar the twist angle departure at the critical field can take both signs; i.e., the system is described by a supercritical bifurcation.

The profile of $\varphi_0(\zeta)$ can be obtained from the relation

$$\zeta = \frac{1}{2}\frac{\int_0^{\varphi_0} \frac{d\varphi}{\sqrt{\sin^2(\varphi-\varphi_H)-\sin^2(\varphi_M-\varphi_H)}}}{\int_0^{\varphi_M} \frac{d\varphi}{\sqrt{\sin^2(\varphi-\varphi_H)-\sin^2(\varphi_M-\varphi_H)}}}, \tag{3.8}$$

and it is shown in Fig. 9 for several values of magnetic angle φ_H and strength ξ.

Note that as $1/\xi$ increases, in the bulk φ_0 tends to φ_H. The deformation is localized close to the boundaries, over a surface layer whose thickness is of the order of ξ.

The total energy per unit surface $\mathcal{G}_0$ is then given by

$$\mathcal{G}_0 = \frac{4}{\xi}\int_0^{\varphi_M} \sqrt{\sin^2(\varphi-\varphi_H)-\sin^2(\varphi_M-\varphi_H)}\,d\varphi - 4\frac{\pi}{\lambda}\varphi_M + \left(\frac{\pi}{\lambda}\right)^2 - \frac{1}{\xi^2}\cos^2(\varphi_M-\varphi_H), \tag{3.9}$$

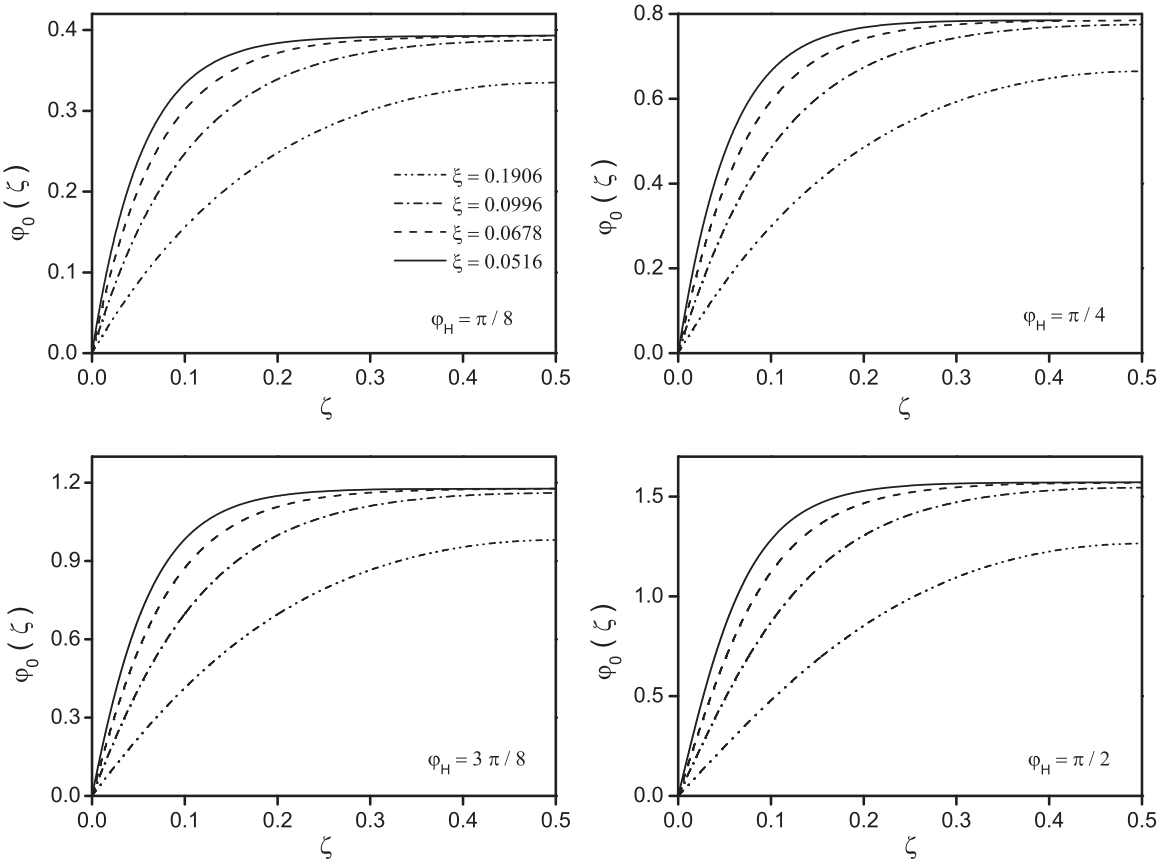

FIG. 9. Shape of $\varphi_0(\zeta)$ for several values of magnetic angle φ_H and strength ξ.

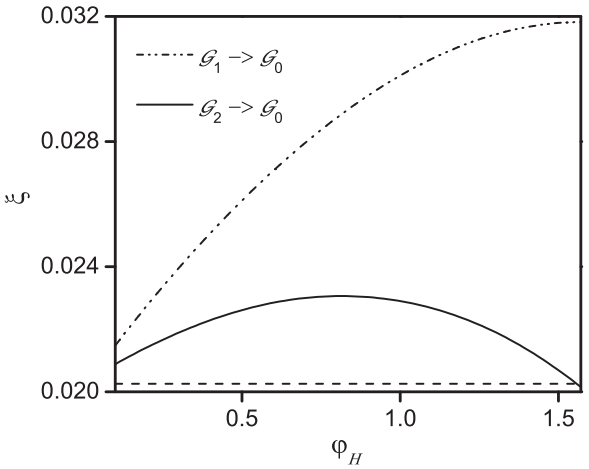

FIG. 11. Dependence of transitions $\mathcal{G}_1 \rightarrow \mathcal{G}_0$ and $\mathcal{G}_2 \rightarrow \mathcal{G}_0$ vs the magnetic angle φ_H, in the case $\lambda = 0.1$. The dashed horizontal line represents the critical coherent length for the case corresponding to a magnetic field parallel to the surface easy direction.

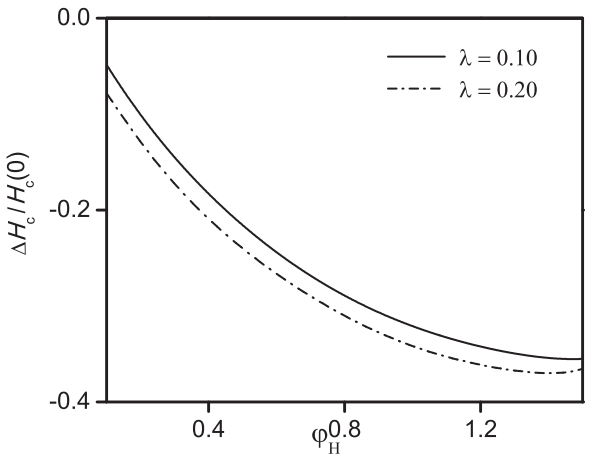

FIG. 12. Relative variation of the critical field for the unwinding the cholesteric liquid chrismal vs φ_H for two different values of the sample thickness.

and is shown in Fig. 10 for the same values of φ_H reported in Fig. 9.

Again we remark on the presence of the anomaly in the curve for $\varphi_H = \pi/2$.

As cited above, the transition from the state presenting n twist to the one having $n-1$ twist takes place when $\mathcal{G}_n \rightarrow \mathcal{G}_{n-1}$, as discussed in Sec. II. Since k_n does not depend on φ_H, the transitions occur at the same critical fields shown in Fig. 4. However, the "final" transition between the state presenting 1 twist on the state 0 takes place when $\mathcal{G}_1 \rightarrow \mathcal{G}_0$. Since $\mathcal{G}_0$ depends on φ_H, the critical magnetic field at the inset of the last transition depends on φ_H too.

This is shown in the final Fig. 11, where we depict the dependence of transitions $\mathcal{G}_1 \rightarrow \mathcal{G}_0$ and $\mathcal{G}_2 \rightarrow \mathcal{G}_1$ versus the magnetic angle φ_H. As is shown, the former takes place at a energy value higher than the latter, a fact that ensures that the cascade $2 \rightarrow 1 \rightarrow 0$ always occurs. In the same figure, we report also the critical coherent length relevant to the case $\varphi_H = 0$. In Fig. 12 the relative variation of the critical field for the unwinding the cholesteric liquid crystal versus φ_H is plotted for two different values of half-twists (i.e., for different thickness of the sample). We note that the influence of φ_H on the critical field is less and less important as the thickness of the sample increases. In the particular case for $\ell \rightarrow \infty$, the critical field will be independent of φ_H since in this case all the directions of the magnetic field, perpendicular to the helical axes, are equivalents.

IV. CONCLUSION

We investigated in a unified way the cholesteric pitch transitions of a finite size sample that are induced by an external bulk field perpendicular to the axis of the helix. We treated the general problem of oblique configuration, i.e., the case of a field tilted in respect to the easy axis direction imposed by the limiting surfaces with strong anchoring conditions. The predicted unwinding of the helix by the field is stepwise and takes place at constant pitch between successive transitions in accord with experimental results [33]. The obtained nematic-cholesteric transition phase diagram reveals the role of the surface field on the transition. The unwinding process leads to the formation of untwisted zones in which the nematic director is practically parallel to the field. The latter zones are separated by π walls where the twist concentrates [Fig. 2(c)]. The accumulation of elastic energy at the π walls should induce a mechanism for the expulsion of the deformation such as continuous unwinding of the helix [39], defect-mediated expulsion, or even a local melting to the isotropic phase. The investigation of creation and propagation of solitary waves should also shed light on the pitch unwinding mechanism. Further, the study of the oblique configuration revealed that the critical fields for all the transitions but the last one do not depend on the tilt angle. In contrast the critical field of the last transition depends on the tilt angle and on the thickness of the sample (Fig. 11), and its value is higher in the parallel configuration. Finally, in the perpendicular configuration a normal bifurcation is evidenced that corresponds to the Fredericks instability of a nematic cell.

In the present paper we assumed that the thickness of the sample is equal to an integer number of the cholesteric half-pitch period. The case of a sample thickness that is incommensurate with the cholesteric half-pitch and the extension toward finite anchoring conditions is the natural extension of the present model.

[1] P. G. de Gennes and J. Prost, *The Physics of Liquid Crystals* (Clarendon Press, Oxford, 1993).
[2] L. M. Blinov, *Structure and Properties of Liquid Crystals* (Springer, Netherlands, 2010).
[3] G. Chilaya, in *Chirality in Liquid Crystals*, edited by H. Kitzerow and C. Bahr, Chap. 6 (Springer, New York, 2001).
[4] P. G. de Gennes, Solid State Commun. **6**, 163 (1968).
[5] R. B. Meyer, Appl. Phys. Lett. **12**, 281 (1968).

[6] E. S. Sackmann, S. Meiboom, and L. C. Snyder, J. Am. Chem. Soc. **89**, 5981 (1967).
[7] J. Wysocki, J. Adams, and W. Haas, Phys. Rev. Lett. **20**, 1025 (1968); **21**, 1791 (1968).
[8] G. Durand, L. Leger, I. Rondelez, and M. Veyssie, Phys. Rev. Lett. **22**, 227 (1969).
[9] R. B. Meyer, Appl. Phys. Lett. **14**, 208 (1969).
[10] F. J. Kahn, Phys. Rev. Lett. **24**, 209 (1970).
[11] H. Baessler and M. M. Labes, Phys. Rev. Lett. **21**, 1791 (1968).
[12] C. J. Gerritsma and P. Van Zanten, Phys. Lett. A **42**, 127 (1972).
[13] R. Dreher, Solid State Commun. **13**, 1571 (1973).
[14] S. V. Belyaev and L. M. Blinov, JETP Lett. **30**, 99 (1979).
[15] V. A. Belyakov, I. W. Stewart, and M. A. Osipov, Phys. Rev. E **71**, 051708 (2005).
[16] A. D. Kiselev and T. J. Sluckin, Phys. Rev. E **71**, 031704 (2005).
[17] P. E. Cladis and M. Kléman, Mol. Cryst. Liq. Cryst. **16**, 1 (1972).
[18] M. Luban, D. Mukamel, and S. Shtrikman, Phys. Rev. A **10**, 360 (1974).
[19] P. J. Kedney and I. W. Stewart, Lett. Math. Phys. **31**, 261 (1994).
[20] P. J. Kedney and I. W. Stewart, Continuum Mech. Thermodyn. **6**, 141 (1994).
[21] V. A. Belyakov and E. I. Kats, JETP **91**, 488 (2000).
[22] V. A. Belyakov, JETP Lett. **76**, 88 (2002).
[23] P. Oswald, J. Baudry, and S. Pirkl, Phys. Rep. **337**, 67 (2000).
[24] R. Seidin, D. Mukamel, and D. W. Allender, Phys. Rev. E **56**, 1773 (1997).
[25] B. Regaya, J. Prost, and H. Gasparoux, Rev. de Phys. Appl. **7**, 83 (1972).
[26] J. S. Patel and R. B. Meyer, Phys. Rev. Lett. **58**, 1538 (1987).
[27] Sin-Doo Lee, J. S. Patel, and R. B. Meyer, J. Appl. Phys. **67**, 1293 (1990).
[28] H. A. van Sprang and J. L. M. van de Venne, J. Appl. Phys. **57**, 175 (1985).
[29] E. Niggemann and H. Stegemeyer, Liq. Cryst. **5**, 739 (1989).
[30] L. J. M. Schlangen, A. Pashai, and H. J. Cornelissen, J. Appl. Phys. **87**, 3723 (2000).
[31] W. C. Yip and H. S. Kwok, Appl. Phys. Lett. **78**, 425 (2001).
[32] I. I. Smalyukh, B. I. Senyuk, P. Palffy-Muhoray, O. D. Lavrentovich, H. Huang, E. C. Garland, V. H. Bodnar, T. Kosa, and B. Taheri, Phys. Rev. E **72**, 061707 (2005).
[33] H. G. Yoon, N. W. Roberts, and H. F. Gleeson, Liq. Cryst. **33**, 503 (2006).
[34] S. T. Lagerwall, *Ferroelectric and Antiferroelectric Liquid Crystals* (Wiley-VCH, New York, 1999).
[35] M. D. Betterton and F. Jülicher, Phys. Rev. E **71**, 011904 (2005).
[36] J. Gore, Z. Bryant, M. Nöllmann, M. U. Le, N. R. Cozzarelli, and C. Bustamante, Nature **442**, 836 (2006).
[37] F. Ritort, J. Phys. Condens. Matter **18**, R531 (2006).
[38] I. Lelidis and P. Galatola, Phys. Rev. E **66**, 010701 (2002).
[39] P. S. Salter, G. Carbone, S. A. Jewell, S. J. Elston, and P. Raynes, Phys. Rev. E **80**, 041707 (2009).